Published in final edited form as:

Curr Biol. 2011 October 25; 21(20): 1685–1694. doi:10.1016/j.cub.2011.08.049.

The Tubulin Deglutamylase CCPP-1 Regulates the Function and Stability of Sensory Cilia in *C. elegans*

Robert O'Hagan[1], **Brian P. Piasecki**[2], **Malan Silva**[1], **Prasad Phirke**[2], **Ken C.Q. Nguyen**[3], **David H. Hall**[3], **Peter Swoboda**[2], and **Maureen M. Barr**[1]

[1]Department of Genetics, Rutgers, The State University of New Jersey, Piscataway, NJ 08854

[2]Karolinska Institute, Center for Biosciences at NOVUM, Department of Biosciences and Nutrition, Hälsovägen 7, S-141 83 Huddinge, Sweden

[3]Center for *C. elegans* Anatomy, Albert Einstein College of Medicine, 1410 Pelham Parkway, Bronx NY 10461

Summary

Background—Post-translational modifications (PTMs) such as acetylation, detyrosination, and polyglutamylation have long been considered markers of stable microtubules, and have recently been proposed to guide molecular motors to specific subcellular destinations. Microtubules can be deglutamylated by the cytosolic carboxypeptidase CCP1. Loss of CCP1 in mice causes cerebellar Purkinje cell degeneration. Cilia, which are conserved organelles that play important diverse roles in animal development and sensation, contain axonemes comprised of microtubules that are especially prone to PTMs.

Results—Here, we report that a CCP1 homolog, CCPP-1, regulates the ciliary localization of the kinesin-3 KLP-6 and the polycystin PKD-2 in male-specific sensory neurons in *C. elegans*. In male-specific CEM (cephalic sensilla, male) cilia, *ccpp-1* also controls the velocity of the kinesin-2 OSM-3/KIF17 without affecting the transport of kinesin-II cargo. In the core ciliated nervous system of both males and hermaphrodites, loss of *ccpp-1* causes progressive defects in amphid and phasmid sensory cilia, suggesting that CCPP-1 activity is required for ciliary maintenance but not ciliogenesis. Affected cilia exhibit defective B-tubules. Loss of TTLL-4, a polyglutamylating enzyme, suppresses progressive ciliary defects in *ccpp-1* mutants.

Conclusions—Our studies suggest that CCPP-1 acts as a tubulin deglutamylase that regulates the localization and velocity of kinesin motors, and the structural integrity of microtubules in sensory cilia of a multicellular, living animal. We propose that the neuronal degeneration caused by loss of CCP1 in mammals may represent a novel ciliopathy in which cilia are formed but not maintained, depriving the cell of cilia-based signal transduction.

Corresponding Author: Maureen Barr, Department of Genetics, Rutgers, The State University of New Jersey, Piscataway, NJ 08854. barr@biology.rutgers.edu. Phone: (732) 445-1639 Fax: (732) 445-1147.

Introduction

Cilia are microtubule-based organelles that are present on most non-dividing eukaryotic cells and are essential for vision, olfaction, hearing, and embryonic development [1]. Ciliary axonemes typically have a "9 + 2" or "9 + 0" microtubule (MT) formation (nine outer doublets with two inner singlets, or nine outer doublets, with zero inner singlets), but variations do occur [1].

All motile and non-motile eukaryotic cilia are built by a process called IFT (intraflagellar transport) [2]. Anterograde IFT is driven by heterotrimeric kinesin-II motors that transport IFT-A and IFT-B complexes [2]. This basic IFT machinery can be accompanied by other accessory motors. *C. elegans* amphid channel cilia are built by the cooperative action of two kinesin-2 motors—homodimeric kinesin-2 OSM-3 and heterotrimeric kinesin-II, comprised of KLP-11, KLP-20, and KAP-1 [2, 3]. In *C. elegans* male-specific CEM cilia, the kinesin-3 KLP-6 moves independently of the IFT kinesin-2 motors and reduces the velocity of OSM-3 [4]. In humans, mutations that affect cilia formation or function can cause genetic diseases called ciliopathies that display pleiotropic defects, including cystic kidneys, retinal photoreceptor degeneration, anosmia, and sperm immotility [2].

Ciliary axonemal MTs are subject to post-translational modifications (PTMs). PTMs are considered to be markers of stable microtubules, and can regulate the activities of kinesin and dynein motors [5–8]. For example, kinesin-3/KIF1A localization to axons and dendrites is regulated by the level of MT polyglutamylation [9]. At present, our understanding of the physiological relevance of tubulin PTMs is very limited.

We report here several ciliary defects arising from a mutation in the gene *ccpp-1*, which encodes a cytosolic carboxypeptidase tubulin modifying enzyme. The *ccpp-1(my22)* mutant was isolated in a genetic screen for defective ciliary localization of PKD-2::GFP, a functional fluorescently tagged TRP polycystin ion channel [10]. The murine homolog, CCP1 (also called Nna1 or AGTPBP1) is a deglutamylating enzyme that reduces the polyglutamylation that is added as a side chain to glutamate residues in the C-terminus of tubulin [11]. CCP1 also removes the penultimate amino acid, a glutamate, encoded in the primary sequence of tubulin to produce Δ2-tubulin [11].

C. elegans ccpp-1 mutants also displayed defects in localization of the kinesin-3 KLP-6, and abnormal motility of OSM-3/KIF17 in male-specific cilia required for mating behavior. In amphid and phasmid neurons, loss of CCPP-1 function caused progressive ciliary dye-filling (Dyf) defects, suggesting that ciliary structure is not maintained. The progressive Dyf defect in *ccpp*-1 mutants was dependent on the TTLL-4 polyglutamylase. *ccpp-1* animals also displayed cell-specific defects in ciliary polyglutamylation signals. Our results provide the first demonstration that CCPP-1 regulates the function and stability of neuronal cilia. Loss of function of CCP1 in *pcd* mice causes progressive degeneration of cerebellar Purkinje neurons, thalamic neurons, retinal photoreceptors, and olfactory mitral neurons, as well as sperm immotility [12, 13], phenotypes that are reminiscent of human ciliopathies. We propose that CCPP-1 affects the structure and stability of ciliary MTs, the function of ciliary

kinesins, and ciliary localization of their cargoes, by regulating the polyglutamylation state of ciliary MTs.

Results

my22 and *ok1821* are alleles of *ccpp-1,* which is required for proper localization of PKD-2::GFP

We isolated the *my22* allele in a screen for ciliary PKD-2::GFP localization defective mutants [10]. PKD-2::GFP localizes to cilia located on the distal dendrites of CEMs, RnBs, and HOB male-specific neurons (Fig. 1A, B) [14]. In *my22* males, excessive PKD-2::GFP accumulates in cilia and distal dendrites (hereafter referred to as the Cil phenotype; Fig. 1B) [10].

We mapped *my22* to a region between +0.39 and +0.5 cM on chromosome I. The Cil phenotype in *my22* mutants was rescued by germline injection of fosmid WRM0627dB11, which contains full genomic sequence of seven genes, of which only the *ccpp-1(ok1821)* mutant failed to complement *my22* for the Cil phenotype. *ccpp-1(ok1821)* males also displayed the Cil phenotype, which was rescued by a genomic *ccpp-1(+)* transgene (Fig. 1B). We conclude that both *my22* and *ok1821* are recessive alleles of a single gene, *ccpp-1*.

The *my22* molecular lesion affects a conserved domain in CCPP-1

The *my22* lesion is a G-A transition encoding a G596R amino acid substitution (Fig. 1C) in the conserved sequence FESGNL (Fig. 1C). The *ccpp-1(ok1821)* mutation encodes a deletion that removes putative 5′ regulatory sequences as well as the first 5 exons of the *ccpp-1* locus, and may be a genetic null (Fig. 1C). BLASTs [15] of *C. elegans* CCPP-1 against human sequences revealed several conserved domains, including a zinc carboxypeptidase domain ([16]; Fig. 1C), and showed that residues 536 – 1015 are 43% identical to human CCP1 residues 573 – 1122. Hence, *ccpp-1* encodes an evolutionarily conserved protein.

CCPP-1::GFP is expressed in the ciliated sensory nervous system

We analyzed expression and localization of a *ccpp-1::gfp* translational reporter. CCPP-1::GFP was neuronally expressed in developing embryos (not shown) through adulthood in amphid and IL2 ciliated sensory neurons of the "core" nervous system, which males and hermaphrodites have in common (Fig. 1D, E). In the male-specific nervous system, CCPP-1::GFP was coexpressed with *pkd-2* in CEM head neurons and the B-type ray (RnB) and HOB hook neurons in the tail (Fig 1E). CCPP-1::GFP was also expressed in some unidentified neurons and the gubernacular erector and retractor muscles in the male tail (Fig. 1E). CCPP-1::GFP was localized diffusely throughout neurons, including cilia, but excluded from the nucleus.

To determine if CCPP-1::GFP was functional, we assayed the mating behavior of transgenic males. *ccpp-1* mutant males are defective in the response substep of mating (Fig. 1F; [10]), in which males sense contact with and begin scanning the body of a potential hermaphrodite mate [17]. Response behavior requires the ray neurons [14, 18]. While 99 ± 1% of wild-type

males (7 trials, $n = 70$ animals total assayed) responded to hermaphrodite mates within four minutes, only 38 ± 8% of *ccpp-1(my22)* (4 trials, $n = 40$) and 35 ± 9% of *ccpp-1(ok1821)* males responded (6 trials, $n = 60$) (Fig. 1F). Genomic *ccpp-1(+)* and *ccpp-1::gfp* transgenes rescued the response defect in *ccpp-1* mutant males (Fig. 1F). Hence, the CCPP-1::GFP translational fusion protein was functional in RnB neurons.

ccpp-1 mutants exhibit a progressive defect in ciliary structure

We performed dye-filling assays to assess the structural integrity of cilia in the amphid and phasmid sensillae of *ccpp-1* mutants [19]. Wild-type amphid and phasmid ciliated sensory neurons took up a lipophilic fluorescent dye through environmentally exposed ciliated endings (Fig. 2 A, B; [19]). Mutants with ciliary structure defects, such as *osm-3(p802)* and the IFT-B polypeptide mutant *che-13(e1805)* exhibit the Dyf phenotype at all developmental stages [19]. *ccpp-1(ok1821)* hermaphrodites displayed an age-dependent Dyf defect (Fig. 2 A, B). In young *ccpp-1* larvae (L1 or L2), amphid dye-uptake appeared nearly normal (Fig. 2B), while L4 larvae and young adults (YA) showed a severe Dyf phenotype in ciliated sensory neurons in both the amphid and phasmid sensillae. Older adults displayed the most severe Dyf phenotype. *ccpp-1(my22)* hermaphrodites displayed a similar, but less penetrant, age-dependent Dyf defect (Fig. 2 B), consistent with *ok1821* being a loss-of-function and *my22* being a reduction-of-function allele. The Dyf phenotype in *ccpp-1(ok1821)* animals at all ages was rescued by a *ccpp-1(+)* transgene (Fig. 2 B).

C. elegans relies on ciliated sensory neurons of the amphid sensilla to detect and avoid high osmolarity [20]. Cilium structure mutants, such as *che-13(e1805)*, are osmotic avoidance defective (the Osm phenotype) at all developmental stages (Fig. 2C; [19, 20]). *ccpp-1* mutants exhibited progressive Osm defects that mirrored the progressive Dyf phenotype (Fig. 2C). *ccpp-1(ok1821)* L1 and L2 larvae were slightly defective (avoidance index, or a.i., of 0.80 ± 0.06; $p < 0.0001$ versus 1.0 ± 0 for wild-type; Fig. 2C), but this defect became more severe with age (a.i. = 0.23 ± 0.01 of 1–2 day old adults; $p < 0.0001$ versus 0.99± 0.04 for wild type; Fig. 2C). As adults, *ccpp-1(my22)* mutants were also partially defective in osmotic avoidance behavior (Fig. 2D). In all cases, the Osm phenotype of *ccpp-1* mutants was fully rescued by the *ccpp-1::gfp* transgene (Fig. 2D). Based on the results of dye-filling and osmotic avoidance assays, which reflect the structure and function of amphid cilia, we propose that *ccpp-1* mutants are capable of forming but not maintaining sensory cilia.

ccpp-1 mutants display ciliary ultrastructural defects including B-tubule defects, disorganization of MTs, and ciliary fragmentation

To examine the ultrastructure of the CEM and amphid cilia, we used transmission electron microscopy (TEM) and electron tomography of fixed age-matched young adult males. Wild-type CEM cilia typically contained approximately 20 singlet MTs that were distributed spatially, with many singlets closely apposed to the membrane, when viewed in cross section (Fig. 3A; Table 1). CEM cilia in a *ccpp-1(ok1821)* male contained only 16 MT singlets on average, and those that remained were disorganized, residing on average four times farther from the membrane than in wild type (Fig. 3A; Table 1). The average diameter of *ccpp-1(ok1821)* CEM cilia was 66% larger than wild type (Fig. 3A; Table 1).

In wild-type males, the amphid channel middle segment region contained ten axonemes and each contained on average eight visible outer microtubule doublets (Fig. 3B; Table 1). In a *ccpp-1(ok1821)* male, the amphid channel middle segment region contained an average of only eight intact cilia that had on average two outer doublets and few singlets, which appeared disorganized (Fig. 3B; Table 1). Some of the singlets appeared to have attached remnants of B-tubules. Some missing cilia may have fragmented (Fig. 3B; Table 1). Hence, CCPP-1 function is important for ciliary integrity as well as MT architecture.

CCPP-1 regulates polyglutamylation in sensory cilia

Murine CCP1 removes the penultimate amino acid, a glutamate, of the primary sequence of α-tubulin and shortens side chains of glutamates (polyglutamylation) added to the C-terminus of α- and β-tubulins in stable microtubules [11]. CCPP-6 was reported to reduce polyglutamylation in *C. elegans* sensory cilia [21].

If *ccpp-1* Cil and Dyf defects were caused by excessive glutamylation of ciliary MTs, loss of a polyglutamylase might suppress *ccpp-1* defects. Polyglutamylases—enzymes that oppose deglutamylases—are known as tubulin tyrosine ligase like (TTLL) proteins [22, 23]. The *C. elegans* genome encodes six predicted TTLL homologs [21]. In *C. elegans* core ciliated sensory neurons, *ttll-4* mutants display drastically reduced antibody detection of polyglutamation signals in cilia, while *ttll-9* mutants show a minor reduction [21]. IFT70/DYF-1 positively regulates polyglutamylation in *C. elegans* and zebrafish [24]. To determine if mutations in *ttll-4*, *ttll-9*, or *dyf-1* could suppress *ccpp-1* Cil or Dyf phenotypes, we examined double mutant combinations. Strikingly, *ttll-4(tm3310)* suppressed the progressive Dyf, but not Cil, phenotype of *ccpp-1(ok1821)* mutants (Fig. 4A, B, Fig. S1). *ttll-9(tm3389)* did not suppress *ccpp-1* Cil or Dyf phenotypes (data not shown). Our results indicate that CCPP-1 opposes the activity of TTLL-4 in polyglutamylation of proteins in amphid and phasmid cilia. Both the *dyf-1(mn335)* single mutant and *dyf-1(mn335) ccpp-1(my22)* double mutant were Dyf and Cil (Fig. S1). Because *dyf-1* and *ccpp-1* single and double mutants display similar Dyf and Cil phenotypes, we cannot draw any conclusion about genetic interactions between them.

To detect polyglutamylation, we stained adult males with the monoclonal antibody GT335 [25]. In wild type, GT335 neuronal staining was most apparent in the middle segments of amphid cilia, IL cilia in the nose, and phasmid cilia in the tail (Fig. 4C). GT335 occasionally stained the CEM cilia in males, as visualized by PKD-2::GFP (Fig. 4D, S2A). GT335 stained the distal tips of male tail ray neuronal cilia (Fig. 4C). *ccpp-1* mutations had cell-type specific effects on polyglutamylation. In general, GT335 immunofluorescence appeared to be more speckled in *ccpp-1* mutants (Fig. 4C). *ccpp-1(my22)* and *ccpp-1(ok1821)* showed an approximately five-fold increase over wild type in the percent of CEM cilia with GT335 staining (Fig. 4D, S2A). Increased polyglutamylation in *ccpp-1* CEM cilia is consistent with CCPP-1 acting as a deglutamylase. Not surprisingly, the increased polyglutamylation in CEM cilia was not suppressed in *ccpp-1(ok1821);ttll-4(tm3310)* or *dyf-1(mn335) ccpp-1(my22)* double mutants (Fig. S2A, B).

In contrast, peak GT335 staining of amphid middle segments in *ccpp-1* adult males was significantly reduced to half or less of wild type (Fig. 4E, S2C). GT335 fluorescence in

phasmid cilia of the tail and in male ray neuronal cilia also appeared to be decreased in *ccpp-1* mutants (Fig. 4C). In some cases, ray neurons appeared to retain low polyglutamylation signals, but these signals were in ciliary bases rather than the tips of cilia (Fig. 4C inset). The reduction of polyglutamylation in *ccpp-1* mutants was unexpected, but might reflect the ciliary ultrastructural defects in *ccpp-1* adults. In *ccpp-1(ok1821);ttll-4(tm3310)* and *dyf-1(mn335) ccpp-1(my22)* double mutants, the reduction in polyglutamylation signals in amphid middle segments was similar to the *ccpp-1* single mutants (Fig. S2B, C). Since both TTLL-4 and DYF-1 positively regulate polyglutamylation, this result was expected.

To determine if *ccpp-1* mutations perturbed other PTMs, we examined polyglycylated tubulin and Δ2-tubulin by antibody staining. The *C. elegans* genome lacks predicted polyglycylating enzymes [21]; as expected, we detected no polyglycylation signals (data not shown). An anti-Δ2-tubulin polyclonal antibody stained pairs of lateral neurites in wild-type males, but did not stain cilia except the phasmids in the tail; Fig. S2D). In *ccpp-1* mutants, the anti-Δ2-tubulin antibody also dimly stained some cilia in the nose (Fig. S2D).

CCPP-1 regulates the kinesin-3 KLP-6 and the kinesin-2 OSM-3

To determine if *ccpp-1* regulates the abundance or localization of ciliary motor proteins, we examined KLP-6, OSM-3/KIF17, and the kinesin-II cargo OSM-6. In wild type, KLP-6::GFP is diffusely localized throughout neuronal cell bodies, axons, dendrites, and cilia of the male-specific CEM, HOB, and RnB neurons and the core IL2 neurons (Fig. 5A; [26]). In *ccpp-1(my22)* mutants, KLP-6::GFP accumulated in cilia (Fig. 5A). We used the *pkd-2* promoter to drive expression of *ccpp-1* in the male-specific CEM, HOB, and RnB neurons [27], which rescued KLP-6::GFP abundance and localization in cilia of these neurons (Fig. 5B, C). We conclude that CCPP-1 acts cell-autonomously to regulate the distribution of KLP-6 and its putative cargo, PKD-2.

Next, we investigated OSM-3 in CEM cilia for two reasons: First, we could observe the effects of *ccpp-1(ok1821)* on OSM-3::GFP motility and localization in a single cilium, whereas the amphid channel contains cilia of 8 different neuronal types [19]. Second, TEM experiments indicated that amphid cilia in *ccpp-1* mutants had variable structural defects (Fig. 3), indicating that individual amphid channel cilia might be affected differently or with different timecourses. In CEM cilia, the majority of OSM-3 moves independently of kinesin-II and IFT complexes [4]. The localization of OSM-3::GFP was similar in wild type and *ccpp-1(ok1821)* CEM cilia (Fig. 6A). However, the apparent velocity of motile OSM-3::GFP puncta in CEM cilia was significantly increased in *ccpp-1(ok1821)* mutants (1.07 ± 0.07 μm/s vs. 0.75 ± 0.03 μm/s; Fig. 6B). Mutation of *ttll*-4 had no effect on OSM-3::GFP localization or velocity in either wild-type or *ccpp*-1 backgrounds (Fig. S3A, B, C), consistent with the failure of *ttll-4* to suppress the Cil phenotype of *ccpp-1*.

OSM-6 is an IFT-B polypeptide that is transported solely by kinesin-II in CEM cilia [4]. *ccpp-1(ok1821)* did not affect abundance, localization, or velocity of OSM-6::GFP (Fig. 6C, D, S3D). We conclude that, in CEM cilia, CCPP-1 regulates the accessory motors OSM-3 and KLP-6, but does not regulate the canonical IFT motor, heterotrimeric kinesin-II.

Discussion

Loss of CCPP-1 function causes ciliary transport defects and progressive deterioration of ciliary structure and function

Here we show that the *C. elegans* carboxypeptidase CCPP-1 plays critical cell-specific roles in maintaining ciliary integrity and function *in vivo*. *ccpp-1* mutants are defective in localization and abundance of the kinesin-3 KLP-6 and its putative cargo PKD-2 in male-specific sensory cilia. Mutant males also have a corresponding mating defect in response behavior, which requires PKD-2 and KLP-6 function [14, 26]. Unlike IFT mutants, *ccpp-1* mutant larvae exhibit amphid cilia that fill with dye and support osmotic avoidance behavior. However, *ccpp-1* mutants display a progressive, age-dependent dye-filling defect of cilia in amphid and phasmid sensory neurons, which correlates with deficits in osmotic avoidance behavior. We propose that CCPP-1 is needed for ciliary maintenance rather than ciliogenesis. Two previous studies have shown that CCP1 requires a functional carboxypeptidase domain to rescue defects in *pcd* mice [28, 29]. The *ccpp-1(my22)* mutation, which encodes a G596R substitution, demonstrates that the FESGNL motif is also essential for full function (Fig. 1B). However, the function of this domain, or indeed, the CCPP-1 protein itself, is not fully understood.

CCPP-1 regulation of the tubulin code affects specific kinesin motors

Our results are consistent with a proposed "tubulin code" model, in which PTMs provide signposts that regulate the localization or activity of motors [5–8]: In male-specific CEM cilia of *ccpp-1* mutants, ciliary localization of KLP-6 is elevated, and the apparent velocity of OSM-3::GFP is increased. In contrast, the localization and motility of the kinesin-II-driven IFT-B polypeptide OSM-6::GFP are unaffected. We propose that CCPP-1-mediated MT modification normally regulates KLP-6 subcellular distribution and OSM-3 velocity in CEM cilia. Identification of additional roles for CCPP-1, such as regulating dynein-based transport, motor recycling, or cargo-motor binding, await future studies.

CCPP-1 regulates MT polyglutamylation, MT stability, and ciliary stability

In CEM cilia, CCPP-1 regulates polyglutamylation levels independently of TTLL-4 (Fig. 4, S1, S2A, B, S3C). We suggest that polyglutamylation in CEM cilia is normally maintained at a low level by CCPP-1 and an unknown TTLL polyglutamylase. Since misregulation of MT polyglutamylation affects the kinesin-2 OSM-3 and the kinesin-3 KLP-6, we propose that the PKD-2::GFP Cil phenotype could be secondary to motor function defects. Our data strongly suggest that CCPP-1 reduces polyglutamylation of MTs and opposes polyglutamylating enzymes in *C. elegans* cilia.

Our results also predict that CCPP-1 activity depends on cell-specific factors, since loss of TTLL-4 suppresses *ccpp-1* Dyf, but not Cil, defects. Such cell-specific factors may include particular tubulin isoforms or regulators of PTMs. In amphid cilia, mutation of *ccpp-1* decreases polyglutamylation levels (Fig. 4, S2C)—counter to our expectation, considering that mammalian CCP1 deglutamylates MTs, and that loss of the polyglutamylase TTLL-4 suppressed the Dyf phenotype of *ccpp-1* mutants. However, hyperglutamylation destabilizes axonemal MTs in *Tetrahymena* [30]. Degradation of extensively polyglutamylated MTs, as

well as the loss of some amphid cilia, might explain the paradoxical loss of GT335 staining in amphid cilia middle segments in *ccpp-1* adults.

Our ultrastructural studies support this hypothesis (Fig. 3B, Table 1). In *ccpp-1* amphid cilia, the number of both doublets and singlets is reduced by 75% compared to wild type (Table 1). In *Chlamydomonas* ciliary MT doublets, B-tubules are the main site of polyglutamylation [31]. Assuming this is true in *C. elegans*, the B-tubule defects we observed are likely to explain the reduction of GT335 staining in *ccpp-1* amphid cilia. These ultrastructural defects are also consistent with the progressive Dyf phenotype in *ccpp-1* mutants. We propose that the degree of polyglutamylation must be tightly controlled for MT doublet stability.

Does mutation of CCP1 in mammals cause ciliopathic neurodegeneration?

A greater understanding of the function of CCPP-1 is of interest because the mammalian homolog, CCP1, is required for survival of several populations of neurons in the mouse brain [12, 13]. In addition to adult-onset degeneration of cerebellar Purkinje neurons, other defects, such as degeneration of retinal photoreceptors, olfactory bulb mitral neurons, and thalamic neurons, and sperm immotility, result from loss of CCP1 [12, 13]. All of the cell types affected in *pcd* mice are ciliated/flagellated. RNAi-mediated knockdown of CCP1 reduced ciliary length in cultured human cells [32]. We show here, for the first time, that CCPP-1 is required for maintenance of the structure and function of cilia in *C. elegans.*

Consequently, we propose that neurodegeneration and other defects in *pcd* mice could be caused by ciliopathy. Vertebrate primary cilia may be specialized for intercellular signaling such as Wnt and Hedgehog (reviewed in [33]). In addition to developmental roles, such signaling might be needed for cellular survival and maintenance of cilia in which receptors reside. Hence, further study of *ccpp-1*, tubulin post-translational modification, and ciliary dynamics in *C. elegans* should provide more insight on ciliopathic degenerative diseases.

Experimental Procedures

Strains used

The genotypes of all strains used are described in Supplemental Experimental Procedures.

PKD-2::GFP Localization

Strains used: PT443, PT1645, PT1931, PT1932, PT2168, PT2169, PT2170, PT2171, PT2172, PT2379, PT2381—We isolated L4 males from hermaphrodites 20 – 24 hours before observation. To score the Cil phenotype, we observed PKD-2::GFP localization on the Zeiss Axioplan2 microscope using the 10X objective. At this magnification, GFP fluorescence was not visible anywhere outside of the cell bodies of the CEM, RnB, or HOB neurons in wild-type males. In *ccpp-1* mutants, PKD-2::GFP was visible in dendrites and cilia, especially in rays. Images of PKD-2::GFP localization were captured using 63X or 100X objectives.

Antibody Staining

Strains used: PT443, PT1645, PT2168, PT2171, PT2172, PT2379, PT2381— Gravid adults were bleached to obtain age-synchronized embryos, which were then fixed as one-day-old adults. We used the fixation and staining method described in [34]). Fixed worms were stored at 4°C for up to one month before antibody staining. Animals were stained overnight at room temperature with a 1:600 dilution in Antibody Buffer A of GT335 (a monoclonal antibody which binds the branch point of both monoglutamylated and polyglutamylated substrates [25]); 1:500 dilution of AB3203 (polyclonal antibody that binds Δ2-tubulin; Millipore; [37]); 1:200 dilution of TAP952 (monoclonal antibody that binds both mono-glycylated and polyglycylated tubulin, a gift from the Drummond laboratory); and a 1:200 dilution of R2302 anti-poly-G (rabbit polyclonal antibody that binds polyglycylated tubulin, a gift from the Gorovsky laboratory). Alexa Fluor-578-conjugated anti-mouse or anti-rabbit secondary antibodies (Invitrogen) were used at a dilution of 1:2000 and incubated for 2 hours at room temp with gentle agitation. See Supplemental Experimental Procedures for details.

Statistical Methods

All data values are expressed as mean ± standard error unless indicated. To determine the statistical significance of differences in experimental results, we conducted statistical tests in IGOR 6 (Wavemetrics, Inc.), Statplus (Analystsoft), or Prism (Graphpad Software).

See Supplemental Experimental Methods

C. elegans culture, mapping of *my22* mutation, transgenesis, microscopy, KLP-6::GFP localization, OSM-3::GFP and OSM-6::GFP motility, male mating response behavior, dye-filling and osmotic avoidance behavior, and electron microscopy and tomography.

Supplementary Material

Refer to Web version on PubMed Central for supplementary material.

Acknowledgments

This work was supported by: NIH NRSA 5F32NS56540-4 and NJCSCR 10-2951-SCR-E-0 fellowships to RO; a Fulbright Fellowship and a Lars Hiertas Minne Foundation grant to BPP; NIH RO1DK059418 to MBB; grants from the Swedish Research Council, Marcus Borgström Foundation, and the NordForsk Nordic Networks for *C. elegans* and Cilia/Centrosomes Research to PS; NIH RR12596 to DHH; and Einstein funds for access to the NYSBC. We thank Bill Rice and K.D. Derr (New York Structural Biology Center) for help in using the Technai20 microscope, and creating electron tomograms. Some nematode strains used in this work were provided by the Caenorhabditis Genetics Center, which is funded by the NIH National Center for Research Resources (NCRR); The *C. elegans* Gene Knockout Consortium; and the National Bioresource Project for the Nematode (Japan). Thanks to the Drummond and Gorovsky laboratories for the anti-polyglycylation antibodies. We also thank Natalia Morsci, Andrew Jauregui, and Julie Maguire for plasmids and strains, and members of the Barr laboratory for discussions and constructive criticism of this manuscript.

References

1. Fliegauf M, Benzing T, Omran H. When cilia go bad: cilia defects and ciliopathies. Nat Rev Mol Cell Biol. 2007; 8:880–893. [PubMed: 17955020]
2. Scholey JM. Intraflagellar transport motors in cilia: moving along the cell's antenna. J Cell Biol. 2008; 180:23–29. [PubMed: 18180368]

3. Pan X, Ou G, Civelekoglu-Scholey G, Blacque OE, Endres NF, Tao L, Mogilner A, Leroux MR, Vale RD, Scholey JM. Mechanism of transport of IFT particles in *C. elegans* cilia by the concerted action of kinesin-II and OSM-3 motors. J Cell Biol. 2006; 174:1035–1045. [PubMed: 17000880]
4. Morsci NS, Barr MM. Kinesin-3 KLP-6 Regulates Intraflagellar Transport in Male-Specific Cilia of Caenorhabditis elegans. Curr Biol. 2011; 21:1239–1244. [PubMed: 21757353]
5. Bulinski JC, Gundersen GG. Stabilization of post-translational modification of microtubules during cellular morphogenesis. BioEssays : news and reviews in molecular, cellular and developmental biology. 1991; 13:285–293.
6. Verhey KJ, Gaertig J. The tubulin code. Cell Cycle. 2007; 6:2152–2160. [PubMed: 17786050]
7. Janke C, Kneussel M. Tubulin post-translational modifications: encoding functions on the neuronal microtubule cytoskeleton. Trends Neurosci. 2010; 33:362–372. [PubMed: 20541813]
8. Ikegami K, Setou M. Unique post-translational modifications in specialized microtubule architecture. Cell Struct Funct. 2010; 35:15–22. [PubMed: 20190462]
9. Ikegami K, Heier RL, Taruishi M, Takagi H, Mukai M, Shimma S, Taira S, Hatanaka K, Morone N, Yao I, et al. Loss of alpha-tubulin polyglutamylation in ROSA22 mice is associated with abnormal targeting of KIF1A and modulated synaptic function. Proc Natl Acad Sci U S A. 2007; 104:3213–3218. [PubMed: 17360631]
10. Bae YK, Lyman-Gingerich J, Barr MM, Knobel KM. Identification of genes involved in the ciliary trafficking of *C. elegans* PKD-2. Dev Dyn. 2008; 237:2021–2029. [PubMed: 18407554]
11. Rogowski K, van Dijk J, Magiera MM, Bosc C, Deloulme JC, Bosson A, Peris L, Gold ND, Lacroix B, Grau MB, et al. A family of protein-deglutamylating enzymes associated with neurodegeneration. Cell. 2010; 143:564–578. [PubMed: 21074048]
12. Fernandez-Gonzalez A, La Spada AR, Treadaway J, Higdon JC, Harris BS, Sidman RL, Morgan JI, Zuo J. Purkinje cell degeneration *(pcd)* phenotypes caused by mutations in the axotomy-induced gene, Nna1. Science. 2002; 295:1904–1906. [PubMed: 11884758]
13. Mullen RJ, Eicher EM, Sidman RL. Purkinje cell degeneration, a new neurological mutation in the mouse. Proc Natl Acad Sci U S A. 1976; 73:208–212. [PubMed: 1061118]
14. Barr MM, DeModena J, Braun D, Nguyen CQ, Hall DH, Sternberg PW. The *Caenorhabditis elegans* autosomal dominant polycystic kidney disease gene homologs *lov-1* and *pkd-2* act in the same pathway. Curr Biol. 2001; 11:1341–1346. [PubMed: 11553327]
15. Altschul SF, Gish W, Miller W, Myers EW, Lipman DJ. Basic local alignment search tool. Journal of molecular biology. 1990; 215:403–410. [PubMed: 2231712]
16. Rodriguez de la Vega M, Sevilla RG, Hermoso A, Lorenzo J, Tanco S, Diez A, Fricker LD, Bautista JM, Aviles FX. Nna1-like proteins are active metallocarboxypeptidases of a new and diverse M14 subfamily. Faseb J. 2007; 21:851–865. [PubMed: 17244817]
17. Liu KS, Sternberg PW. Sensory regulation of male mating behavior in *Caenorhabditis elegans*. Neuron. 1995; 14:79–89. [PubMed: 7826644]
18. Barrios A, Nurrish S, Emmons SW. Sensory regulation of *C. elegans* male mate-searching behavior. Curr Biol. 2008; 18:1865–1871. [PubMed: 19062284]
19. Perkins LA, Hedgecock EM, Thomson JN, Culotti JG. Mutant sensory cilia in the nematode *Caenorhabditis elegans*. Dev Biol. 1986; 117:456–487. [PubMed: 2428682]
20. Culotti JG, Russell RL. Osmotic avoidance defective mutants of the nematode *Caenorhabditis elegans*. Genetics. 1978; 90:243–256. [PubMed: 730048]
21. Kimura Y, Kurabe N, Ikegami K, Tsutsumi K, Konishi Y, Kaplan OI, Kunitomo H, Iino Y, Blacque OE, Setou M. Identification of tubulin deglutamylase among *Caenorhabditis elegans* and mammalian cytosolic carboxypeptidases (CCPs). J Biol Chem. 2010; 285:22936–22941. [PubMed: 20519502]
22. Janke C, Rogowski K, Wloga D, Regnard C, Kajava AV, Strub JM, Temurak N, van Dijk J, Boucher D, van Dorsselaer A, et al. Tubulin polyglutamylase enzymes are members of the TTL domain protein family. Science. 2005; 308:1758–1762. [PubMed: 15890843]
23. Ikegami K, Mukai M, Tsuchida J, Heier RL, Macgregor GR, Setou M. TTLL7 is a mammalian beta-tubulin polyglutamylase required for growth of MAP2-positive neurites. J Biol Chem. 2006; 281:30707–30716. [PubMed: 16901895]

24. Pathak N, Obara T, Mangos S, Liu Y, Drummond IA. The zebrafish *fleer* gene encodes an essential regulator of cilia tubulin polyglutamylation. Molecular biology of the cell. 2007; 18:4353–4364. [PubMed: 17761526]
25. Wolff A, de Nechaud B, Chillet D, Mazarguil H, Desbruyeres E, Audebert S, Edde B, Gros F, Denoulet P. Distribution of glutamylated alpha and beta-tubulin in mouse tissues using a specific monoclonal antibody, GT335. European journal of cell biology. 1992; 59:425–432. [PubMed: 1493808]
26. Peden EM, Barr MM. The KLP-6 kinesin is required for male mating behaviors and polycystin localization in *Caenorhabditis elegans*. Curr Biol. 2005; 15:394–404. [PubMed: 15753033]
27. Barr MM, Sternberg PW. A polycystic kidney-disease gene homologue required for male mating behaviour in *C. elegans*. Nature. 1999; 401:386–389. [PubMed: 10517638]
28. Wang T, Parris J, Li L, Morgan JI. The carboxypeptidase-like substrate-binding site in Nna1 is essential for the rescue of the Purkinje cell degeneration (*pcd*) phenotype. Mol Cell Neurosci. 2006; 33:200–213. [PubMed: 16952463]
29. Chakrabarti L, Eng J, Martinez RA, Jackson S, Huang J, Possin DE, Sopher BL, La Spada AR. The zinc-binding domain of Nna1 is required to prevent retinal photoreceptor loss and cerebellar ataxia in Purkinje cell degeneration (*pcd*) mice. Vision research. 2008; 48:1999–2005. [PubMed: 18602413]
30. Wloga D, Dave D, Meagley J, Rogowski K, Jerka-Dziadosz M, Gaertig J. Hyperglutamylation of tubulin can either stabilize or destabilize microtubules in the same cell. Eukaryotic cell. 2010; 9:184–193. [PubMed: 19700636]
31. Kubo T, Yanagisawa HA, Yagi T, Hirono M, Kamiya R. Tubulin polyglutamylation regulates axonemal motility by modulating activities of inner-arm dyneins. Curr Biol. 2010; 20:441–445. [PubMed: 20188560]
32. Kim J, Lee JE, Heynen-Genel S, Suyama E, Ono K, Lee K, Ideker T, Aza-Blanc P, Gleeson JG. Functional genomic screen for modulators of ciliogenesis and cilium length. Nature. 2010; 464:1048–1051. [PubMed: 20393563]
33. Gerdes JM, Davis EE, Katsanis N. The vertebrate primary cilium in development, homeostasis, and disease. Cell. 2009; 137:32–45. [PubMed: 19345185]
34. Lewis JA, Fleming JT. Basic culture methods. Methods Cell Biol. 1995; 48:3–29. [PubMed: 8531730]
35. Kosugi S, Hasebe M, Tomita M, Yanagawa H. Systematic identification of cell cycle-dependent yeast nucleocytoplasmic shuttling proteins by prediction of composite motifs. Proc Natl Acad Sci U S A. 2009; 106:10171–10176. [PubMed: 19520826]
36. de Castro E, Sigrist CJ, Gattiker A, Bulliard V, Langendijk-Genevaux PS, Gasteiger E, Bairoch A, Hulo N. ScanProsite: detection of PROSITE signature matches and ProRule-associated functional and structural residues in proteins. Nucleic acids research. 2006; 34:W362–365. [PubMed: 16845026]
37. Paturle-Lafanechere L, Eddé B, Denoulet P, Van Dorsselaer A, Mazarguil H, Le Caer JP, Wehland J, Job D. Characterization of a major brain tubulin variant which cannot be tyrosinated. Biochemistry. 1991; 30:10523–10528. [PubMed: 1931974]

Highlights

- *C. elegans* CCPP-1 is needed for maintenance of the structure and function of cilia
- Loss of CCPP-1 causes B-tubule defects in ciliary MT structures
- CCPP-1 regulates ciliary kinesin-2 and kinesin-3 motors, but not kinesin-II
- Loss of polyglutamylase TTLL-4 suppresses progressive ciliary defects of *ccpp-1*

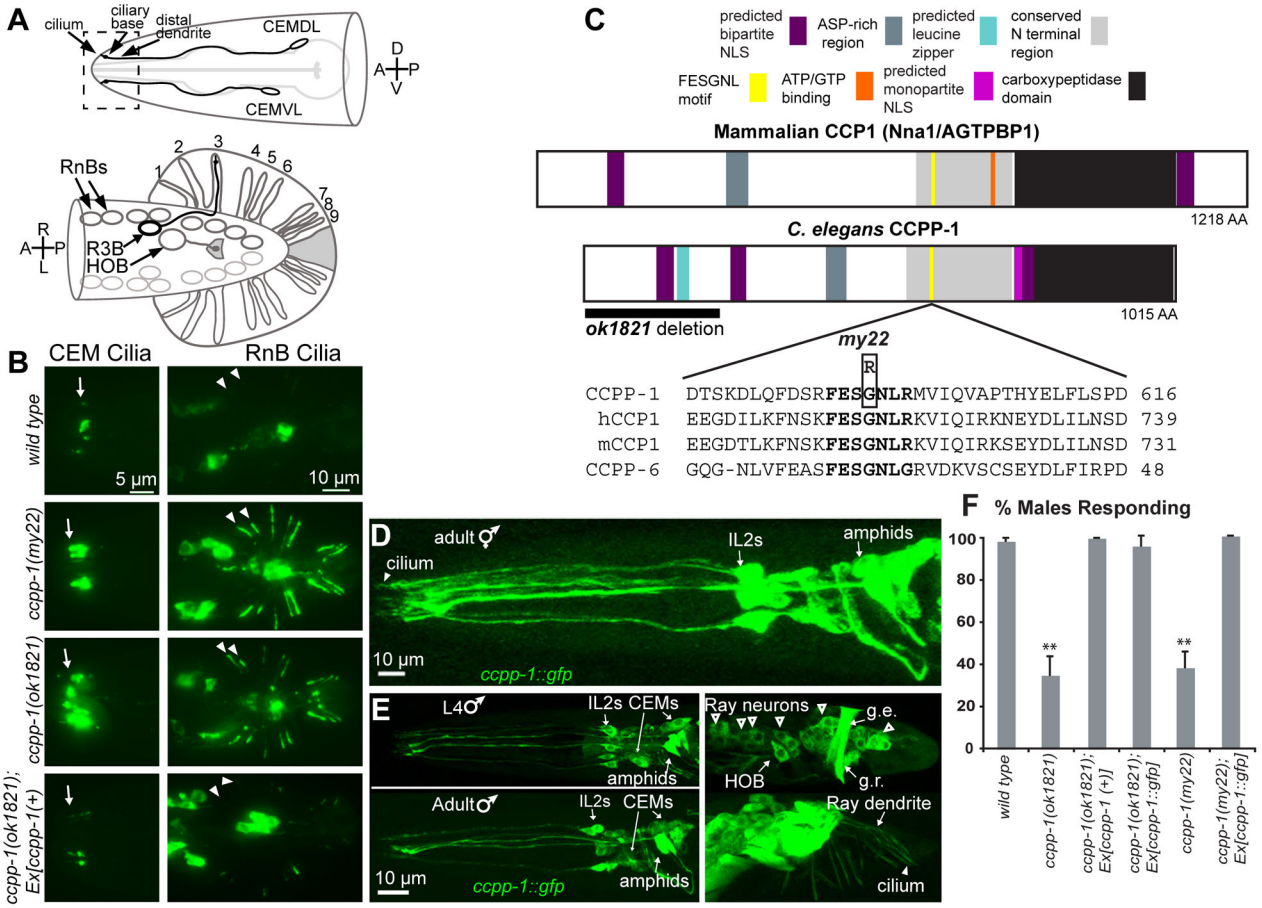

Fig. 1. CCPP-1 is required for PKD-2 localization and is expressed in the ciliated sensory nervous system

A Diagram of the male-specific CEM neurons in the head, and HOB and RnB neurons in the tail. Box illustrates the region of CEM cilia and distal dendrites shown in the epifluorescent images. In the ventral-up cartoon of the male tail, the RnBs innervate the tail rays; R3B dendrite is shown as an example. **B** In wild-type males, PKD-2::GFP faintly illuminated cilia of the CEM neurons, the HOB cilium, and the cilia of the ray B-type neurons (RnB, where n = 1 – 9, excluding 6). *ccpp-1(my22)* and *ccpp-1(ok1821)* mutants exhibit the Cil phenotype. Arrows point to CEM cilia; arrowheads point to R1B and R2B cilia. Expression of genomic *ccpp-1* rescued the Cil phenotype of *ccpp-1(ok1821)*. **C** CCPP-1 contains several conserved regions, including a zinc carboxypeptidase domain, an aspartic-acid rich domain, a conserved "NT" region [12], and predicted NLS (nuclear localization signal; [35]). CCPP-1 also contains a predicted leucine zipper near the N-terminus (ScanProsite, [36]). The *my22* lesion affects the conserved sequence FESGNL in the NT region of CCPP-1. **D** In adult hermaphrodites, CCPP-1::GFP expression was expressed in amphid and IL2 core ciliated sensory neurons. Cilium containing CCPP-1::GFP is indicated. **E** Confocal projections of CCPP-1::GFP expression in males. Top (L4): CCPP-1::GFP was expressed in (left) amphid, IL2, and CEM neurons and (right) male tail ray and HOB neuronal cell bodies (empty arrowheads). Gubernacular erector (g.e.) and retractor (g.r.) muscles are indicated.

Bottom (1 day old adult): CCPP-1::GFP localization in ray neuron dendrites (arrow) and a cilium (arrowhead). **F** *ccpp-1* mutants are defective in response behavior. Number of trials and number of males for each genotype was as follows: wild type, 7 trials, $N = 70$ males; *ok1821*, 6 trials, $N = 60$; *ok1821;Ex[ccpp-1(+)]*, 3 trials, $N = 29$; *ok1821;Ex[ccpp-1::gfp]*, 3 trials, $N = 24$; *my22*, 4 trials, $N = 40$; *my22;Ex[ccpp-1::gfp]*, 5 trials, $N = 39$. Error bars indicate SEM; **indicates *ccpp-1* mutants were statistically different ($p < 10^{-4}$, ANOVA/Tukey HSD test) from mutants expressing *ccpp-1* transgenes, which were similar to wild type. See also Fig. S1.

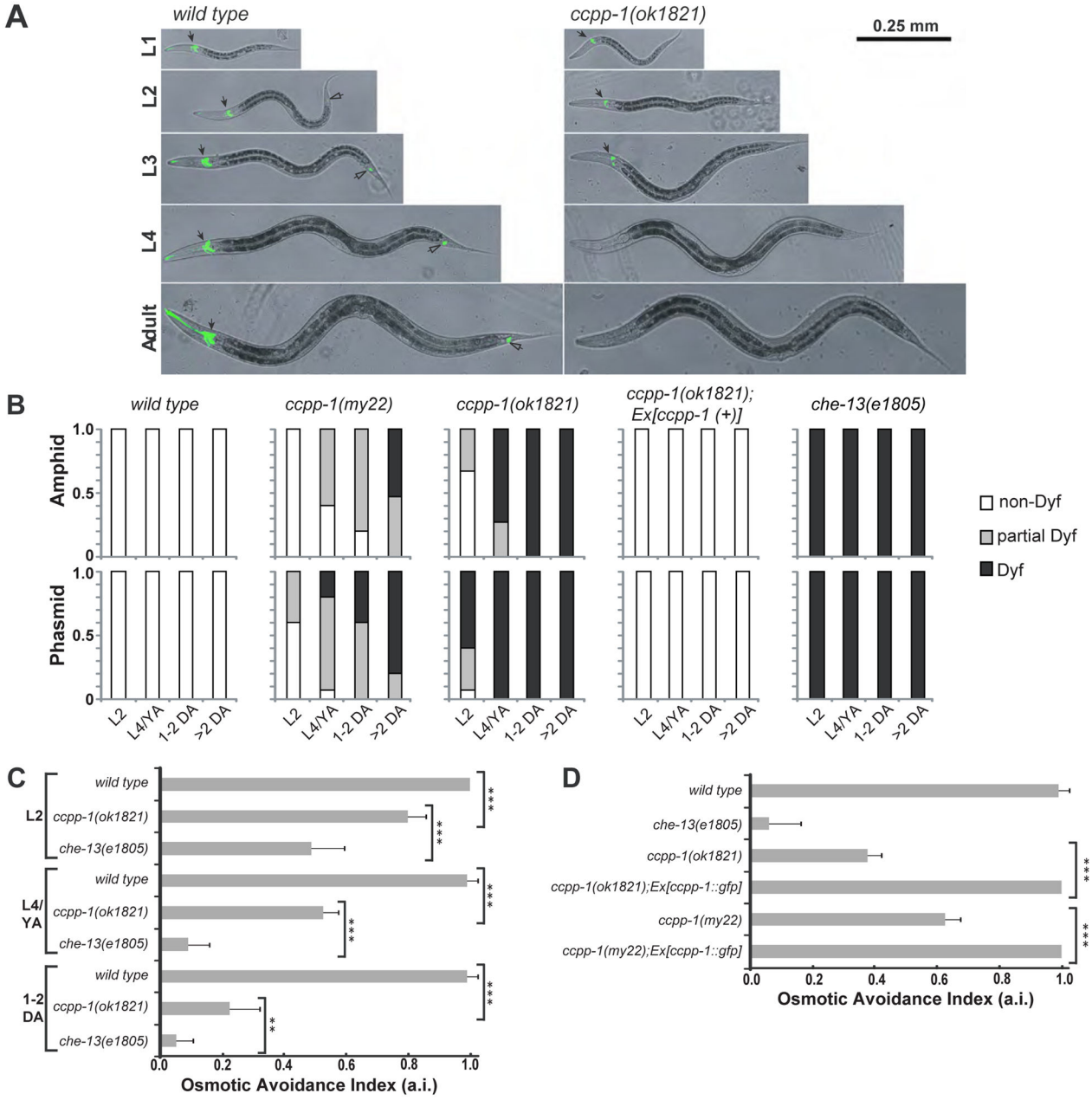

Fig. 2. *ccpp-1* mutants exhibited progressive Dyf and Osm defects

A Amphid (solid arrows) and phasmid (hollow arrows) ciliated neurons of wild type hermaphrodites were stained by DiI (pseudocolored green) at all developmental stages. *ccpp-1(ok1821)* amphid cilia in L1 larvae stained normally, but became Dyf in later larval stages and adults. **B** Dyf defects were scored in amphid and phasmid neurons in wild-type, *my22*, *ok1821*, and *che-13(e1805)* young adults (24 hours post-L4). 15 animals were scored for each stage/genotype. **C** Wild-type animals exhibit osmotic avoidance behavior when challenged with an 8 M glycerol ring. 80 hermaphrodites (8 trials, 10 per trial) were tested for each stage/genotype. Osmotic avoidance index (a.i.) is the fraction of animals that

avoided crossing the ring. **D** The *ccpp-1* Osm defect was rescued by the *ccpp-1::gfp* transgene (8 trials, 10 animals per trial tested). (Error bars indicate SEM; ** indicates p = 0.0022 with Fischer's Exact Test; *** indicates p < 0.0001 with Fischer's Exact Test).

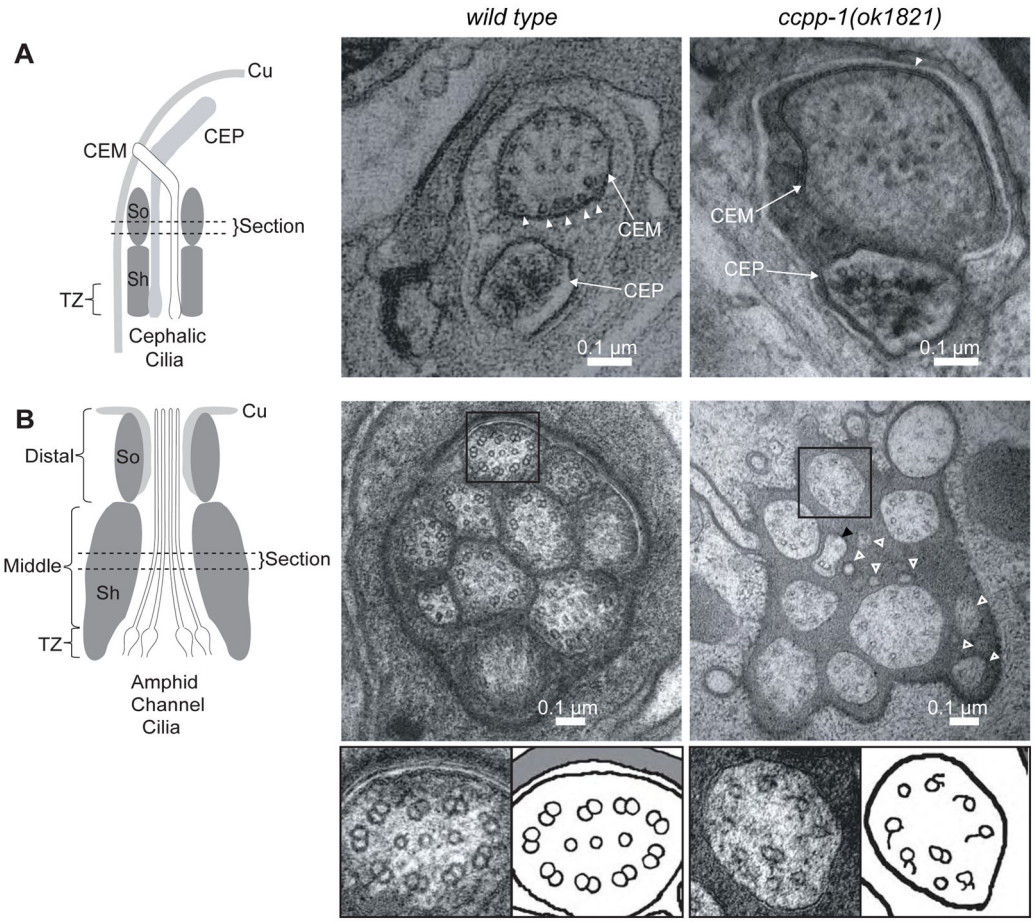

Fig. 3. *ccpp-1(ok1821)* mutants exhibit ciliary ultrastructure defects

Left diagrams show regions from which the cephalic (CEM and CEP) and amphid cilia images were taken (Cu = cuticle; Sh = sheath cell; So = socket cell; TZ =transition zone). **A** EM Images of CEM and CEP cilia in wild-type and *ccpp-1(ok1821)* mutant adult males. Wild-type CEM cilia image (taken from a tomogram) contained many singlet MTs (19 singlets in section shown) closely apposed to the membrane (arrowheads). *ok1821* CEM cilia had fewer singlets (15 singlets in section shown), which were more distant from the membrane (arrowhead indicates one singlet near membrane). The *ok1821* CEM cilium diameter was larger than wild type. **B** Thin sections of amphid cilia in wild-type and *ccpp-1(ok1821)* adult males. Wild-type middle segments contain ten axonemes, each of which typically has nine outer doublets plus a variable number of inner singlets. The *ok1821* middle segment contained only eight intact axonemes plus what appear to be fragments of two cilia (hollow white arrowheads), one of which contains a singlet with attached broken B-tubule (black arrowhead). Most *ok1821* mutant axonemes had fewer MTs, with many doublets replaced by singlets or broken B-tubules. Bottom, boxed wild-type and mutant axonemes accompanied by cartoons. Refer to Table 1 for quantification of images.

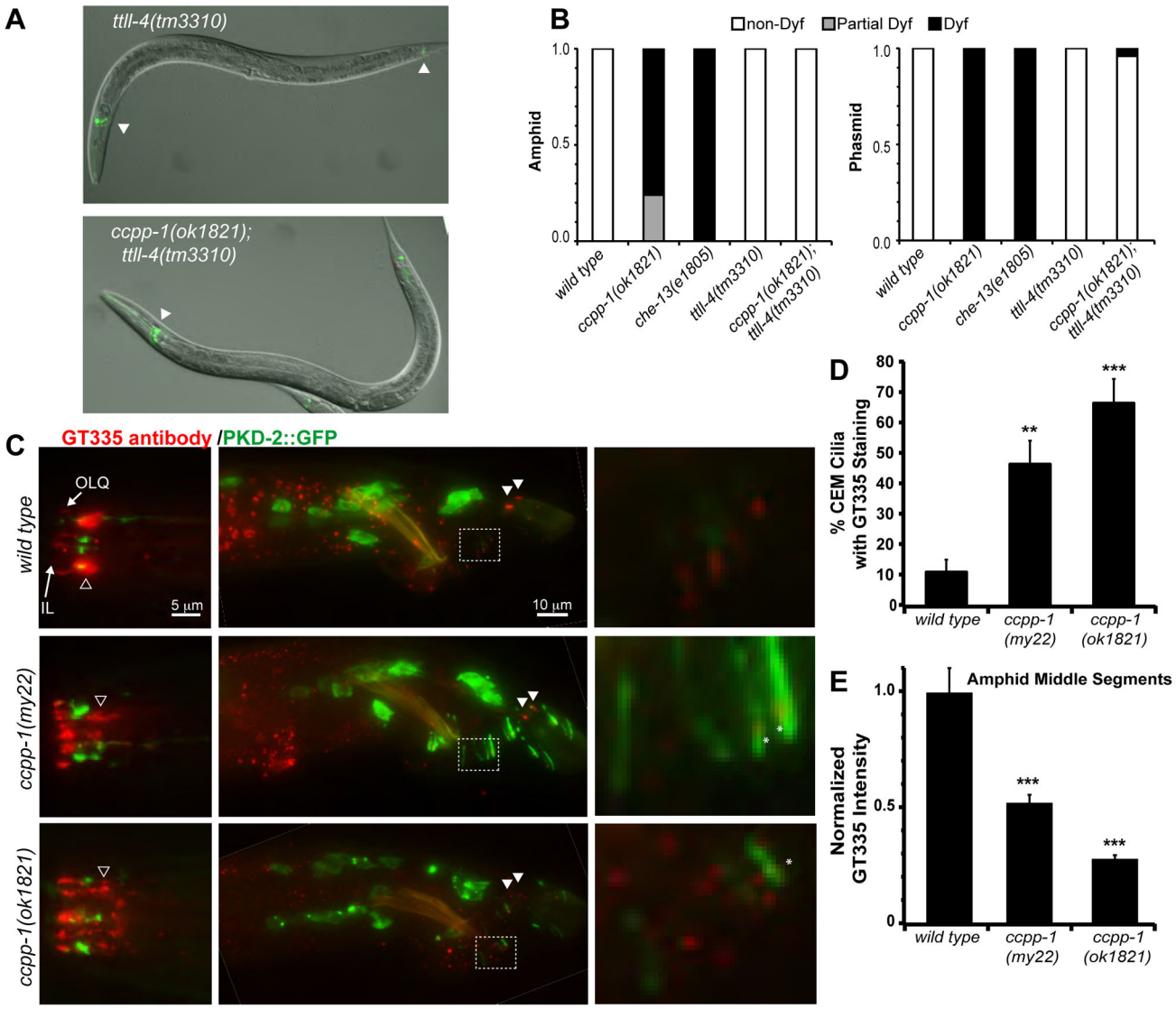

Fig. 4. Loss of CCPP-1 results in altered polyglutamylation of sensory cilia

A Dye uptake (pseudocolored green) was normal in young adult hermaphrodite *ttll-4(tm3310)* mutants (left), which were previously reported to lack polyglutamylation in cilia [21]. Deletion of *ttll-4* suppressed the Dyf phenotype of *ccpp-1* (right). Arrowheads indicate dye-filled amphid and phasmid neurons. **B** Penetrance of Dyf defects in amphid and phasmid neurons. 50 young adult hermaphrodites per genotype were tested. **C** Staining of wild-type and *ccpp-1* mutant young adult males with GT335, a monoclonal antibody that detects polyglutamylation, most prominently in amphid middle segments (hollow arrowhead). An IL and putative OLQ cilium are indicated in the nose. GT335 rarely stained wild-type CEM cilia, which express PKD-2::GFP. In the tail, phasmid cilia (solid arrowheads) were brightly stained. Right, enlarged boxed area containing several ray neuron dendrites and cilia. Asterisks mark polyglutamylation signals that are abnormally localized to the ciliary base in *ccpp-1* mutants. **D** *ccpp-1* mutations increased the incidence of GT335 staining of CEM cilia, which were identified by PKD-2::GFP (** indicates $P < 0.01$, ***

indicates P < 0.001 vs. wild type, ANOVA/Tukey test; *N* = 19 – 22 males per genotype; scored blindly). **E** The normalized peak pixel value of GT335 staining in the area containing amphid middle segments was significantly lower in mutants (Error bars indicate SEM; *** indicates $p < 10^{-5}$ versus wild type, by ANOVA/Tukey HSD test; *N* = 10 males per genotype). See also Fig. S2.

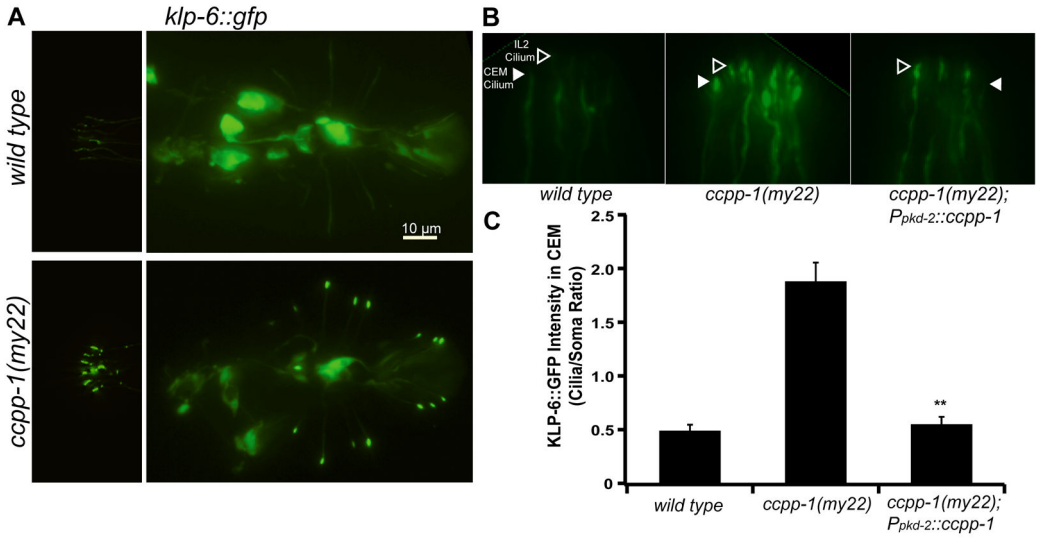

Fig. 5. CCPP-1 is needed for proper localization of KLP-6::GFP in IL2 and male-specific neurons

A KLP-6::GFP localization in IL2 and CEM neurons (left) and in HOB and RnB neurons in the tail (right) is diffuse in wild-type males. In contrast, KLP-6::GFP is highly enriched in cilia in *ccpp-1(my22)* mutants. **B** A magnified view of IL2 (hollow arrowheads) and CEM (solid arrowheads) cilia containing KLP-6::GFP in wild-type, *ccpp-1(my22)*, and *ccpp-1(my22)* rescued young adult males. **C** Quantification of KLP-6::GFP fluorescence in cilia/somata of CEM neurons. KLP-6::GFP localization defects in *ccpp-1(my22)* mutant cilia were rescued by $P_{pkd\text{-}2}$*::ccpp-1* in male specific CEM (and RnB, not shown) neurons (Error bars indicate SEM; $N = 9 – 10$ animals per genotype; ** indicates $P < 0.01$ by t-test versus *ccpp-1(my22)*.)

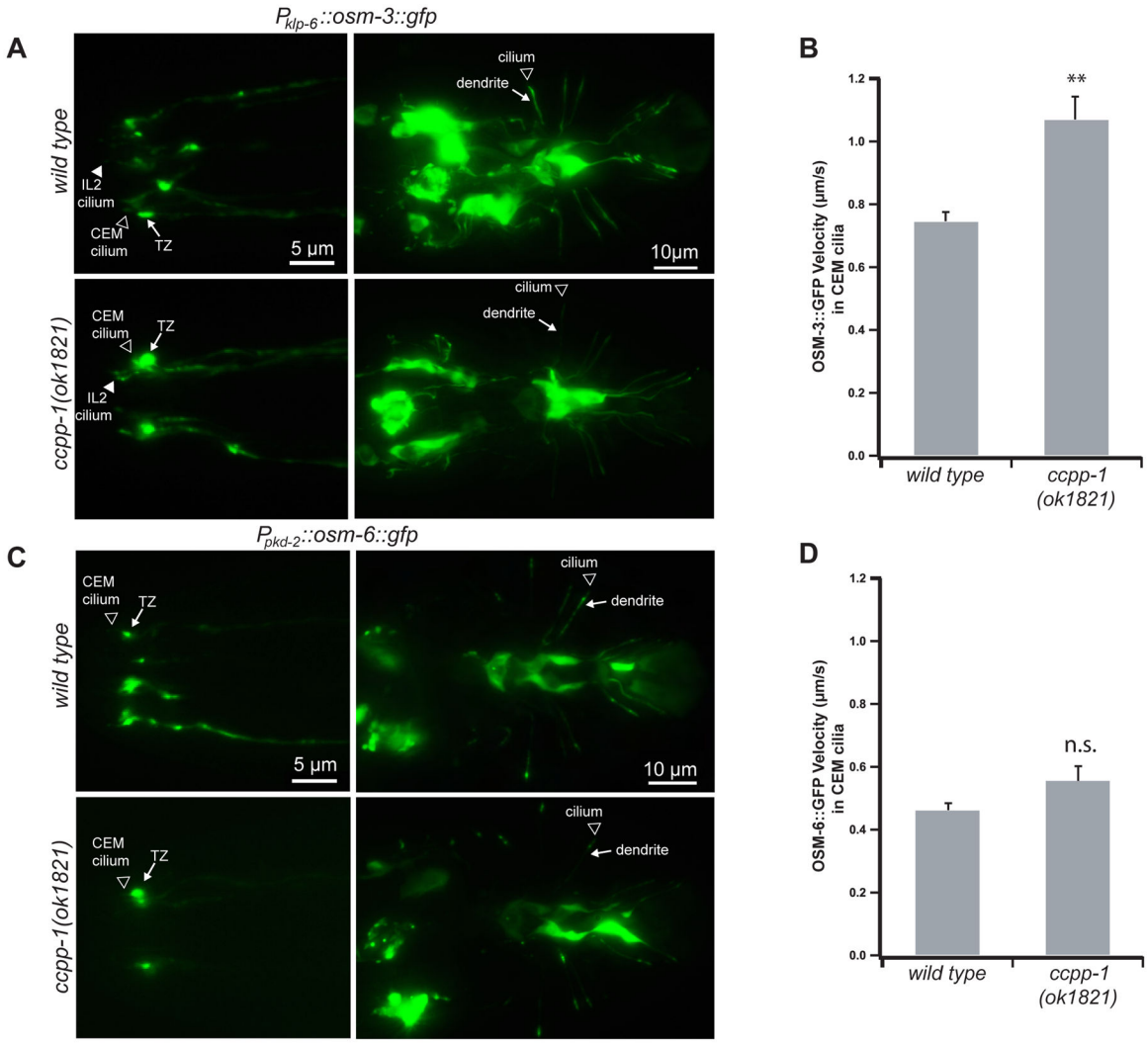

Fig. 6. CCPP-1 regulates the velocity of OSM-3::GFP but not kinesin-II-driven IFT-B polypeptide OSM-6::GFP in CEM cilia

A In wild-type and *ccpp-1(ok1821)* young adult males, *klp-6* promoter-driven OSM-3::GFP was visible diffusely in cell bodies, dendrites, and cilia, with some accumulation in transition zones (TZ). **B** OSM-3::GFP particles moved faster in *ccpp-1* CEM cilia (78 particles in 7 wild-type males; 81 particles in 10 *ccpp-1(ok1821)* males; ** indicates $p < 10^{-4}$ by ANOVA/Tukey test). **C, D** OSM-6::GFP localization and velocity in CEM cilia was similar in wild-type and *ok1821* males (Error bars indicate SEM; 55 particles in 6 wild-type males; 61 particles in 7 *ccpp-1(ok1821)* males; n.s. indicates no significant difference). See also Fig. S3.

Table 1

ccpp-1 mutants display cell-specific defects in ciliary ultrastructure

CEM Cilia	**wild type**	***ccpp-1(ok1821)***
MT singlets per cilium	20 ± 3	16 ± 4
cilium diameter (nm)	230 ± 40	384 ± 45
MT displacement from membrane (nm)	25.1 ± 4.5	99 ± 15**
Amphid Channel Cilia		
cilia per amphid channel	10 ± 0	8.0 ± 1.4
cilia fragments	0 ± 0	3.5 ± 0.7
normal doublets per cilium	8.1 ± 0.9	2.0 ± 0.5**
central singlets	2.4 ± 0.3	0.5 ± 0.2**

We quantified characteristics of CEM cilia and amphid channel cilia middle segments (section is indicated in Fig. 3) from TEM cross-sections and tomographs. For CEM, $n = 3$ cilia per genotype; for amphids, $n = 4$ amphid channels for wild type, $n = 2$ amphid channels for *ok8121*. For number of doublets, 25 wild type and 8 *ok1821* cilia had sufficient resolution in TEM or tomograph images to determine the number of normal doublets and number of singlets; values are average ± SD.

** $P < 0.01$ by Mann-Whitney test.